# Effect of interface evolution on thermal conductivity of vacuum hot pressed SiC/Al composites

# Advanced Engineering Materials

## Effect of interface evolution on thermal conductivity of vacuum hot pressed SiC/Al composites

--Manuscript Draft--

| | |
|---|---|
| **Manuscript Number:** | adem.201400412R1 |
| **Full Title:** | Effect of interface evolution on thermal conductivity of vacuum hot pressed SiC/Al composites |
| **Article Type:** | Full Paper |
| **Section/Category:** | |
| **Keywords:** | Metal-matrix composites (MMCs); thermal conductivity; Interface evolution; Vacuum hot pressing. |
| **Corresponding Author:** | Zhiqiang Li, Ph.D<br>Shanghai Jiao Tong University<br>CHINA |
| **Additional Information:** | |
| **Question** | **Response** |
| Please submit a plain text version of your cover letter here.<br><br>**If you are submitting a revision of your manuscript, please do not overwrite your original cover letter. There is an opportunity for you to provide your responses to the reviewers later; please do not add them here**. | As one of the most promising thermal management materials, SiC/Al composites have been widely studied in interface, which plays an important role to determine the global TC. Interfacial thermal resistance (ITR) between SiC and Al is the key issue since any interface, whatever its state, presents a barrier for thermal exchange. Although interface modification has been studied, the SiC/Al interface evolution, mostly accounting for the variation of ITR, has not been elaborately controlled and characterized, and so far no relevant practical guidance is available in the literatures. In this work, SiC/Al composites were fabricated by a vacuum hot pressing (VHP) process, and the processing parameters were varied to acquire three different kinds of interface configurations, i.e. non-bonded, diffusion-bonded and reaction-bonded interfaces. The as-prepared SiC/Al interface was examined both at the macro- and nanoscale to investigate the presence of interfacial reaction product in particular, and more generally the detailed SiC/Al interface assembly configuration. The effect of interface evolution on global TC of the composites was also investigated and discussed, which would supply a practical guidance for the preparation of highly conductive aluminium matrix composites for thermal management applications. |
| **Corresponding Author Secondary Information:** | |
| **Corresponding Author's Institution:** | Shanghai Jiao Tong University |
| **Corresponding Author's Secondary Institution:** | |
| **First Author:** | Zhizhong Chen |
| **First Author Secondary Information:** | |
| **Order of Authors:** | Zhizhong Chen |
| | Zhanqiu Tan |
| | Gang Ji |
| | Genlian Fan |
| | Dominique Schryvers |
| | Qiubao Ouyang |
| | Zhiqiang Li, Ph.D |
| **Order of Authors Secondary Information:** | |
| **Abstract:** | The SiC/Al composites have been fabricated by a vacuum hot pressing (VHP) process |

| | |
|---|---|
| | in order to study the effect of interface evolution on the global thermal conductivity (TC). By optimizing the VHP parameters of sintering temperature and time, the three different kinds of SiC/Al interface configurations, i.e. non-bonded, diffusion-bonded and reaction-bonded interfaces, are formed and identified by measurement of relative density, X-ray diffraction, scanning and (high-resolution) transmission electron microscopy. The VHPed composite sintered at 655 °C for 60 min is fully dense and presents a tightly-adhered and clean SiC/Al interface at the nanoscale, the ideal diffusion-bonded interface being the most favorable for minimizing interfacial thermal resistance, which in turn results in the highest TC of around 270 W/m K. |

DOI:

# Effect of interface evolution on thermal conductivity of vacuum hot pressed SiC/Al composites**

By *Zhizhong Chen, Zhanqiu Tan**, *Gang Ji, Genlian Fan, Dominique Schryvers, Qiubao Ouyang* and *Zhiqiang Li**

[*] *Mr. Z. Chen, Dr. Z. Tan, Dr. G. Fan, Prof. Q. Ouyang, Prof. Z. Li*
*State Key Laboratory of Metal Matrix Composites*
*Shanghai Jiao Tong University, Shanghai 200240, China*
*E-mail: tanzhanqiu@sjtu.edu.cn; lizhq@sjtu.edu.cn*
*Prof. G. Ji*
*Unité Matériaux et Transformations (UMET) CNRS UMR 8207*
*Université Lille1, 59655 Villeneuve d'Ascq, France*
*Prof. D. Schryvers*
*Electron Microscopy for Materials Science (EMAT), University of Antwerp*
*Groenenborgerlaan 171, 2020 - Antwerp, Belgium*

[**] *The authors would like to acknowledge the financial support of the National Basic Research Program (973 Program) (No. 2012CB619600), the National Natural Science Foundation (Nos. 51071100, 51131004, 51401123), the National High-Tech R&D Program (863 Program) (No. 2012AA030311) and Shanghai Science & Technology Committee (No. 11JC1405500). Dr. Z. Tan also thanks to the Project funded by China Postdoctoral Science Foundation.*

The SiC/Al composites have been fabricated by a vacuum hot pressing (VHP) process in order to study the effect of interface evolution on the global thermal conductivity (TC). By optimizing the VHP parameters of sintering temperature and time, the three different kinds of SiC/Al interface configurations, i.e. non-bonded, diffusion-bonded and reaction-bonded interfaces, are formed and identified by measurement of relative

density, X-ray diffraction, scanning and (high-resolution) transmission electron microscopy. The VHPed composite sintered at 655 °C for 60 min is fully dense and presents a tightly-adhered and clean SiC/Al interface at the nanoscale, the ideal diffusion-bonded interface being the most favorable for minimizing interfacial thermal resistance, which in turn results in the highest TC of around 270 W/m K.

## 1. Introduction

In the microelectronic industry, efficient heat removal has been becoming increasingly urgent for the reliability, energy efficiency and life span of electronic components owing to their increased power density. An electronic component is typically pressed against a heat spreader with high thermal properties to directly dissipate heat. Hence, the development of high-performance thermal dissipation materials has become more and more fascinating, which is also regarded as an indirect solution in addition to new chip design in order to overcome the primary constraint of power density [1]. With light weight, tailored thermal properties and low cost, SiC particles reinforced Al matrix (hereafter referred to as SiC/Al) composites, mainly fabricated by powder metallurgy (PM) and liquid infiltration routes, have been demonstrated as one of the most promising candidates [2-4].

It is well-known that interfaces play an important role to determine global thermal properties of the SiC/Al composites. Poor interfacial bonding can be introduced in the PM composites by incomplete sintering and insufficient interfacial reactions, while excess interfacial reactions involved in the liquid infiltrated composites can introduce a large amount of aluminum carbide ($Al_4C_3$) compound with chemical instability, low thermal and mechanical properties [5-7]. Interfacial

thermal resistance (ITR) between the SiC reinforcement and the Al matrix is an additional issue since any interface, whatever its state, presents a barrier for thermal exchange, however our understanding is very limited on this point.

To achieve high thermal conductivity (TC), two possible processing approaches, i.e. matrix alloying [8, 9] and passive oxidation of SiC particles [10-13], have been attempted in the SiC/Al composites. Matrix alloying by Si element was effective to reduce the excess interfacial reaction between SiC and Al in terms of the equation: $4Al+3SiC \rightarrow Al_4C_3+3Si$. However, such alloying simultaneously lowered the TC of the matrix, which in turn degraded the global TC of the composites. As an example, the TC decreased from 237 W/m K of the SiC/Al to 212 W/m K of the SiC/(Al-11Si) composites, caused by a TC degradation of the matrix itself by around 30 %, from 238 W/m K of the pure Al to 160 W/m K of the Al-11Si alloy [9]. Alternatively, passive oxidation of SiC particles by introducing a thin layer of $SiO_2$ was another way to prevent them from reacting with the Al matrix, which was feasible to achieve good interfacial bonding and mechanical properties. Nevertheless, in this way, the TC of the composites was undesirable due to the high ITR originating from a low TC of $SiO_2$ (only 1.5 W/m K) [11]. In addition, the TC of the composites was also sensitive to thickness variation of the $SiO_2$ layer. For example, the TC decreased from 180 W/m K to 130 W/m K in the passively oxidized SiC/Al composites with increasing the thickness of the $SiO_2$ layer from 0.33 μm to 0.60 μm [10]. More recently, the efforts were also devoted to introduce $MgAl_2O_4$, having a much higher TC (about 50 W/m K) than that of $SiO_2$, by interfacial reaction between $SiO_2$ and Al-Mg alloy [11]. This can play a positive role in improving the TC to some extent, while the ITR remained undesirable since the TC of $MgAl_2O_4$ was only one fourth of that of pure Al matrix (about 230 W/m K). Hence, although proper interface control is a predominant issue

in order to tailor the overall TC of the SiC/Al composites, no relevant practical guidance is available in the literatures.

Our analytical calculations have recently proposed that one of the best ways to improve interfacial bonding as well as to minimize the ITR is to acquire a diffusion-bonded interface (i.e. a tightly adhered interface without or with very few $Al_4C_3$ and, without any additional thermal barrier layers at the nanoscale) by effectively controlling interfacial reaction and formation [14]. In our previous works [15, 16], the diffusion-bonded interface without the excess formation of $Al_4C_3$ were developed in the diamond/Al composites processed by vacuum hot pressing (VHP) with the optimized conditions. It was found that the ITR of the diamond/Al interface ($7.1\times10^{-9}$ $m^2K/W$) in the as-fabricated composites was much lower than that reported from other works ($7.28\times10^{-8}$ $m^2K/W$) [17], and even lower than the ITR measured by a direct method ($2.2\times10^{-8}$ $m^2K/W$) [18], which contributed to a high global TC of around 600 W/m K [15]. Therefore, in this further work and keeping the same practical guidance in mind, the SiC/Al composites were fabricated by varying VHP processing parameters in order to acquire a diffusion-bonded interface. SiC/Al interface of the composites was examined at length scales from the macro to the nanoscale to investigate presence of $Al_4C_3$ in particular and more generally the detailed SiC/Al interface assembly configuration. The effect of interface evolution on global TC of the composites is also investigated and discussed.

## 2．Experimental procedure

An atomized aluminum powder (99.9 % in purity) with a mean size of 75 μm was used as the matrix. It was acquired from Zhejiang Bainianyin Industry and Trade Co.

Ltd., China. A green α-SiC particle (99.4 % in purity) with a mean size of 250 μm was bought from Weifang Kaihua Silicon Carbide Powders Co., Ltd., China, and was used as the reinforcement. Fig. 1 shows that the Al particles have a spherical morphology, while the SiC particles display an irregular shape.

During the processing process, the SiC particles were firstly ultrasonically washed to eliminate possible impurities on the surface. They were then dried and blended with the Al powder with the volume fractions in the range 40-60 vol. % where the 40 vol.% SiC/Al content was used for the optimization of VHP parameters. The powder mixture was cold-pressed at room temperature to acquire a raw billet which was subsequently loaded into a graphite mould and mounted into a VHP unit. The cycle of VHP process illustrated in Fig. 2 includes five steps. The billet was heated up to 400 °C at the rate of 10 °C/min (step A) and held for 30 min for degassing (step B). It was further heated up to the sintering temperature in the range 575-655 °C at the rate of 10 °C/min (step C) and a uniaxial pressure of 68 MPa was simultaneously applied with a sintering time of 15-180 min (step D). After furnace cooling (step E), the VHPed SiC/Al composite specimens with a dimension of Ø12.7×3 mm were obtained. Sintering temperature of the VHP process was measured by two K-type thermocouples located inside the furnace wall, about 20 mm away from the graphite mould.

X-Ray Diffraction (XRD) measurements were performed on a D/max-2550 X-Ray diffractometer, operated at 35 kV/200 mA by using Cu $K_\alpha$ radiation (λ=0.15406 nm), for phase identification. 2θ scans were performed between 20° and 90° with a scan speed of 4 °/min. Careful scanning was performed in the angle range of 30-34° with a step size of 0.05° in order to detect the presence of $Al_4C_3$ (JCPDS file 35-0799). Microstructures at the microscopic and nano-scales were characterized

by scanning electron microscopy (SEM) with a FEI Quanta FEG 250 instrument and (high-resolution) transmission electron microscopy ((HR)TEM) with a FEI Tecnai G2-20 Twin microscope, operated at 200 kV and equipped with a EDAX energy-dispersive X-ray spectroscopy (EDX) analyzer, respectively. TEM thin foils were prepared by mechanical polishing followed by ion milling using a Gatan Model 691 precision ion polishing system. Electron diffraction and fast fourier transformation (FFT) patterns were identified with the aid of JEMS software considering the kinematical approximation.

Relative density was measured by the Archimedes method. TC ($\lambda$) of the VHPed composites at room temperature was calculated from thermal diffusivity ($\alpha$), density ($\rho$) and specific heat capacity ($C_p$) in terms of the equation: $\lambda = \alpha \times C_p \times \rho$. Thermal diffusivity was measured by the laser-flash technique using a Netzsch LFA447 thermal constant analyzer. Each thermal diffusivity value represents an average of three measurements and the standard deviation is 2 %. Specific heat capacity was calculated by the rule of mixtures (ROM) using the specific heat capacity values of the components Al (0.895 J/gK) and SiC (0.660 J/gK).

## 3. Results and discussion

At the given constant uniaxial pressure of 68 MPa, the VHP parameters of sintering temperature and time, in the processing windows of 575-655 °C and 15-180 min, respectively, have been optimized by monitoring evolutions of relative density and TC of the specimens.

### 3.1. Optimization of sintering temperature

As an empirical and preliminary value, the sintering time of 60 min was set in

order to optimize the sintering temperature. Fig. 3 shows the relative density and TC as a function of the sintering temperature of the 40 vol.% SiC/Al composites. The general trend is that both relative density and TC of the composites increase with increase of the sintering temperature. The relative density increases from 94 % at 575 °C to almost 100 % (i.e. full densification) at and above 635 °C, while the TC of the composites increases from 190 W/m K at 575 °C to 267 W/m K at 645 and 655 °C. The TC reaches the maximal value of 267 W/m K only at 645 °C, which is by 10 °C higher than the necessary temperature for full densification at 635 °C. This result indicates that the high TC depends not only on good physical bonding (100 % in relative density) but also on the formation of an ideal interfacial configuration including good chemical bonding and low ITR. The latter is thermodynamically controlled by interfacial diffusion (and/or reaction) in the solid state during the VHP process. The observed temperature difference means the sintering temperature of 645 °C is more beneficial than 635 °C to achieve a higher TC by acquiring an improved interfacial configuration. The maximal TC of the composites is stabilized at the high temperatures of 645°C and 655 °C, which suggests the similar and favorable interfacial configurations in addition to the good physical bonding.

In order to further develop our understanding on interfacial bonding states, facture surface of the composites has been examined. As proved in the diamond/Al composites [16], this can be regarded as an easy and quick method, without delicate mechanical polishing, to indirectly reveal interfacial bonding states by identifying strong and weak SiC/Al interfaces on the fracture surface. As shown in Fig. 4, the composite sintered at 575 °C presents visible pores (arrowed in Fig. 4a) and the SiC particles are loosely embedded in the Al matrix. As a result, this specimen is featured by the weak non-bonded interface. For the composites sintered above 625 °C, neither

pores nor the non-bonded interfaces are observed on the fracture surfaces. In addition, the SiC particles are tightly embedded in the matrix with some SiC particles even fractured ahead of the SiC/Al interface, indicating a strong interfacial bonding. 645°C and 655°C are both favorable for TC and consolidation. However, considering the comprehensive performance of the composite, e.g., mechanical properties (not included in this study), 655 °C was chosen as the optimized sintering temperature.

### 3.2. Optimization of sintering time

Interfacial diffusion is a temperature and time dependent process. In other words, even at the optimized sintering temperature of 655 °C, improper sintering time can still result in a relatively low TC due to insufficient interfacial bonding or excessive interfacial reaction. Evolutions of the relative density and TC of the 40 vol.% SiC/Al composites sintered for 15, 60 and 180 min are shown in Fig. 5. The main benefit by extending the sintering time from 15 min to 60 min is the gain of TC by 19 % from 227 W/m K for 15 min to 269 W/m K for 60 min, while the gain of relative density is marginal from 99.4 % for 15 min to 100 % for 60 min. In this case, the increased TC is clearly attributed to the improved interfacial configurations. Further extension of the sintering time till 180 min has no observable effect on the relative density; also, the global TC stayed the same. It should point out that visible Al seepage occurred severely at 655 °C for 180 min under a uniaxial pressure of 68 MPa due to local melting of Al, so that the volume fraction of SiC in the final composite is increased to about 45 vol.%. Therefore, accordingly, a higher TC should be expected in the composite sintered for 180 min, which is not true here due to the increasing interfacial reaction products with sintering time extending.

To examine the interfacial reaction products, mainly $Al_4C_3$, possibly formed at the high sintering temperature of 655 °C, XRD was performed in all the three sintered

composites, where the XRD patterns of the specimens sintered for 15 and 60 min are very similar and only present the diffracted peaks of Al and SiC. Fig. 6 shows the typical XRD patterns of the specimens sintered for 60 and 180 min. No diffracted peaks of $Al_4C_3$ are detected in the composites sintered for 15 min (XRD pattern not given here) and 60 min indicating the absence or a very limited content of $Al_4C_3$ in the VHPed composites, suggesting a diffusion-bonded interface. Comparatively, the diffracted peaks corresponding to $Al_4C_3$ and Si are identified in the composite sintered for 180 min following the interfacial reaction: $4Al+3SiC \rightarrow Al_4C_3+3Si$. The excessive interfacial reaction thus occurred (i.e. the formation of a reaction-bonded interface) in this sample, which is harmful for the overall TC. However, in this study, the TC of the composite sintered for 180 min is not clearly much lower than that of the counterpart sintered for 60 min, due to the formation of only a few of scattered $Al_4C_3$ and higher SiC volume fraction (about 45 vol.%) caused by Al seepage. It is supposed that once a continuous layer of $Al_4C_3$ was produced between SiC and Al interfaces, e.g. in the liquid infiltrated SiC/Al composites, the TC of the composites would be largely degraded.

### 3.3.Interface evolution at the nanoscale and the calculated ITR

As illustrated in Fig. 7, in terms of the sintering temperature and time used, the different kinds of SiC/Al interface configurations namely, non-bonded, diffusion-bonded and reaction-bonded interfaces are formed, which have a significant impact on the overall TC of the SiC/Al composites. Among them, the non-bonded interface can be easily identified by measuring relative density and examining fracture surface, while the other two interface configurations can be distinguished by XRD at the macroscopic scale, conventional TEM at the sub-micrometer scale and HRTEM at the nanoscale. Fig. 8 shows the tightly-adhered SiC/Al interface of the composite

sintered at 655 °C for 60 min. Very fine dendritic-like stripes at the interface are visible which are extended in the Al matrix. This may provide a hint that initial interfacial reaction may very locally occur at this condition. However, extensive TEM observations by sample tilting and electron diffraction confirm that no well-grown and platelet-like $Al_4C_3$ crystals are present in this sample. HRTEM in Fig. 8b shows that the SiC stacking is seen to be of the 6H type and neither visible pores nor reaction products are present at the interface. Fig. 8c highlights no additional amorphous phase at the interface despite some overlapping of the lattices from both sides. These results do provide direct evidence at the nanoscale of the diffusion-bonded interface as defined above, which is actually the ideal interface to minimize ITR and in turn to maximize the overall TC.

Furthermore, the composite sintered at 655 °C for the longest sintering time of 180 min also shows very good interfacial bonding but with interfacial reaction product of $Al_4C_3$. Fig. 9a shows an $Al_4C_3$ platelet of 300-500 nm in thickness and around 2 μm in length present at the SiC/Al interface. Its nature is confirmed by HRTEM and corresponding FFT pattern shown in Fig. 9b. Compared with the EDX results recorded in the Al matrix (Fig. 9c) and the SiC particle (Fig. 9e), C and Al peaks and a small O peak are revealed in the interfacial platelet (Fig. 9d), which is in accordance with the composition of $Al_4C_3$. The trace of O probably originates from the nanoscale (1-2 nm in thickness) $Al_2O_3$ skin of the as-received Al powder. Due to its hard and non-sintering nature at the present sintering temperature of 655 °C, it can be broken down into small particles and retained surrounding the SiC/Al interface [19]. The (HR)TEM results in Figs. 8 and 9 are in good agreement with that of XRD analyses in Fig. 6. Therefore, the reaction-bonded interface is only formed in the composite sintered at 655 °C for 180 min.

Moreover, the ITR of the SiC/Al composites was calculated using the popular Hasselman-Johnson model [8, 20] in order to better evaluate the effect of interface configurations on the global TC:

$$K_c = \frac{K_m\ 2K_m + K_r^{eff} + 2(K_r^{eff} - K_m)V_r}{2K_m + K_r^{eff} - (K_r^{eff} - K_m)V_r} \quad (1)$$

$$K_r^{eff} = \frac{K_r^{in}}{1 + \frac{K_r^{in}}{\frac{a}{R}}} \quad (2)$$

where subscripts c, *m* and *r* stand for the SiC/Al composite, Al matrix and SiC reinforcement, respectively. *K*, *V*, $a$ and *R* are the global TC experimentally measured, volume fraction, average radius of SiC particles (250 μm) and ITR between the SiC reinforcement and the Al matrix, respectively. Superscript *eff* and *in* denote the effective and intrinsic TC of the SiC reinforcement. As pores are supposed to mainly exist in the Al matrix and can be treated as non-thermally conductive dispersions, the effective TC of the Al matrix can be expressed as:

$$K_m = \frac{K_m^{in}(1 - V_p)}{1 + \frac{1}{2}V_p} \quad (3)$$

where subscript *p* stands for pores. When the values of $K_r^{in}$ and $K_m^{in}$ (375 W/mK [21] and 233 W/mK [8], respectively) were substituted into the above equations, the ITR of the VHPed composites acquired in the different conditions can be calculated. Fig. 10a shows that the ITR values decrease from $4.4\times10^{-7}$ $m^2K/W$ to $4.4\times10^{-8}$ $m^2K/W$ with increasing the sintering temperatures from 575 °C to 655 °C for 60 min. Compared with the TC evolution (Fig. 3b), lower the ITR and higher the TC. Fig. 10b also shows that at the optimized sintering temperature of 655 °C the ITR of the composite sintered for 60 min (having the diffusion-bonded interface) is much lower than that of the composite sintered for 15 min (having the non-bonded interface) and slightly lower than that of the composite sintered for 180 min (having the reaction-bonded

interface). Thus, by considering the effect of the ITR on the TC, the advantage of acquiring the diffusion-bonded interface rather than the reaction-bonded and non-bonded interfaces is clarified experimentally and theoretically.

### 3.4.Comparison of possible interface optimization by different techniques

Technically, it is difficult to form such an ideal diffusion-bonded interface in the SiC/Al composites by other processing processes such as liquid infiltration and spark plasma sintering (SPS). As a result, the liquid infiltrated and SPSed composites generally show the global TCs much lower than those obtained in the VHPed composites fabricated using the optimized condition (i.e. at 655 °C for 60 min) in this work. For comparison, the TC values obtained in this work and those extracted from the previous work in the literatures [2, 3, 8-13, 22] are plotted in Fig. 11(a). The possible reasons responsible for this are linked to the characteristics of the different techniques which are discussed as-follows. On the one hand, the reaction-bonded interface is usually formed in the liquid infiltrated SiC/Al composites due mainly to the excessive formation of $Al_4C_3$ at high processing temperatures usually above 700 $^{\circ}$C, leading to a low TC of 160-235 W/m K [9, 23]. Although some interface modifications were tentatively made by matrix alloying or passive oxidation, the ITR remains very high, as will be discussed in more details in the next paragraph [8-13]. On the other hand, the SPSed SiC/Al composites often show inadequate interfacial bonding since the SPS parameters of relatively low sintering temperature, short sintering time and very rapid heating and cooling rates are usually used. For example, it has been reported that the SPSed 52-58 vol.% SiC/Al composites exhibit a high porosity level of 3.7-12.5 % and

a low TC of 173-208 W/m K[3]. A continuous solid-liquid co-existent state during SPS process was elaborately conducted by alloying of pure Al matrix with a suitable amount of Si in order to improve the interfacial bonding. In this way, the relative density and TC can reach 99 % and 252 W/m K in the 50 vol.% SiC/Al composite, respectively; meanwhile the TC of the matrix is decreased by alloying, which in turn degrades the global TC [2]. In addition, we believe that the use of SPS can most probably result in a heterogeneous interfacial configuration (bonding and ITR) from one SiC/Al interface to another, which could make interface control unfeasible in this case. This basically originates from a locally very large temperature gradient spontaneously generated during the SPS process, being experimentally proved in the fabrication of the hetero-nanostructured (i.e. containing nano-, ultrafine and micrometric grains) Fe-40 at.% Al intermetallics obtained from the milled nanocrystallized powder [24, 25]. Comparatively, the diffusion-bonded interface and high TCs are very accessible in the VHPed composites due first to quite moderate sintering temperature, in between those applied in the liquid infiltration and SPS processes. Second, the sintering time of VHP is usually at least by one order longer than those used in the liquid infiltration and SPS processes.

To further illuminate the advantage of the diffusion-bonded interface formed through VHP process, the ITR values of the SiC/Al composites are compared with those calculated by using original data extracted from previous work, and plotted in Fig. 11b. As can be seen, the VHPed 40-50 vol.%SiC/Al composites, having the ITR values lower than $1\times10^{-7}$ $m^2W/K$ (i.e. formation of the diffusion-bonded interface),

show the highest global TCs (257-287 W/m K, see Fig. 11a). When the content of SiC particles increases in the range of 55-60 vol.%, the ITR of the VHPed composites also increases, which results in decreasing the global TCs by up to 10 %. This result probably reveals technical difficulty and complexity in solid-state sintering of the composites with a high SiC content, which can be related to relatively low density (i.e. local formation of non-bonded interface). Therefore, regarding the global TC of the composites, enough attention should also be paid to other factors such as the particle size, volume fraction and relative density in addition to delicate controlling of diffusion-bonded interface.

## 4. Conclusions

The SiC/Al composites with excellent TCs have successfully been fabricated by conventional VHP process, which enables effective interface control at the nanoscale by adjusting the combination of sintering temperature and time. The large processing window involved in the VHP process allows one to obtain the three kinds of interface configurations i.e., the non-bonded, diffusion-bonded and reaction-bonded interfaces. The non-bonded and reaction-bonded interfaces, due respectively to insufficient sintering and excessive formation of $Al_4C_3$, are harmful to the global TC. However, the diffusion-bonded interfacial state which is featured by a tightly adhered interface without any $Al_4C_3$ is obtained by the optimized sintering parameters (i.e. at 655 °C for 60 min). This ideal interface configuration can minimize the ITR and to achieve the high TC of around 270 W/m K. This study also demonstrates the high potential of the

VHP technique, rather than liquid infiltration and SPS processes to acquire the highly thermal-performance SiC/Al composites for thermal dissipation applications.

Received: ( )
Revised: ( )
Published online: ( )

[1] C. Zweben, 2001 Proceedings International Symposium on: IEEE **2001**, 360.

[2] K. Mizuuchi, K. Inoue, Y. Agari, T. Nagaoka, M. Sugioka, M. Tanaka, T. Takeuchi, J.I. Tani, M. Kawahara, Y. Makino, M. Ito, *Composites Part B* **2012**, 43, 2012.

[3] K. Chu, C. Jia, W. Tian, X. Liang, H. Chen, H. Guo, *Composites Part A* **2010**, 41, 161.

[4] C. Xue, J. Yu, X. Zhu, *Mater. Des.* **2011**, 32, 4225.

[5] S. Peteves, P. Tambuyser, P. Helbach, M. Audier, V. Laurent, D. Chatain, *J. Mater. Sci.* **1990**, 25, 3765.

[6] J.C. Lee, H.I. Lee, J.P. Ahn, J.H. Shim, Z. Shi, *Metall. Mater. Trans. A* **2001**, 32, 1541.

[7] J.C. Lee, H.I. Lee, J.P. Ahn, Z. Shi, Y. Kim, *Metall. Mater. Trans. A* **2000**, 31, 2361.

[8] J. Molina, R. Prieto, J. Narciso, E. Louis, *Scripta Mater.* **2009**, 60, 582.

[9] C. Kawai, *J. Am. Ceram. Soc.* **2001**, 84, 896.

[10] A. Zou, X. Zhou, D. Li, Y. Yu, *Compos. Interface.* **2013**, 20, 107.

[11] C. Xue, J.K. Yu, *Mater. Des.* **2014**, 53, 74.

[12] S. Ren, X. He, X. Qu, Y. Li, *J. Alloys Compd.* **2008**, 455, 424.

[13] J. Liu, Z. Zheng, J. Wang, Y. Wu, W. Tang, J. Lü, *J. Alloys Compd.* **2008**, 465, 239.

[14] Z. Tan, Z. Li, D.B. Xiong, G. Fan, G. Ji, D. Zhang, *Mater. Des.* **2014**, 55, 257.

[15] Z. Tan, Z. Li, G. Fan, X. Kai, G. Ji, L. Zhang, D. Zhang, *Composites Part B* **2012**, 47, 173.

[16] Z. Tan, Z. Li, G. Fan, X. Kai, G. Ji, L. Zhang, D. Zhang, *Diamond Relat. Mater.* **2012**, 31, 1.

[17] K. Chu, C.C. Jia, X.B. Liang, H. Chen, *Int. J. Min. Met. Mater.* **2010**, 17, 234.

[18] R. Stoner, H. Maris, *Phys. Rev. B* **1993**, 48, 16373.

[19] L. Jiang, Z. Li, G. Fan, D. Zhang, *Scripta Mater.* **2011**, 65, 412.

[20] D. Hasselman, K.Y. Donaldson, A.L. Geiger, *J. Am. Ceram. Soc.* **1992**, 75, 3137.

[21] S.L. Shindé, J. Goela, High thermal conductivity materials: *Springer*, **2006**.

[22] S. Ren, X. He, X. Qu, I.S. Humail, Y. Li, *Compos. Sci. Technol.* **2007**, 67, 2103.

[23] L. Weber, G. Sinicco, J. Molina, *J. Mater. Sci.* **2010**, 45, 2203.

[24] G. Ji, F. Bernard, S. Launois, T. Grosdidier, *Mater. Sci. Eng. A* **2013**, 559, 566.

[25] G. Ji, T. Grosdidier, N. Bozzolo, S. Launois, *Intermetallics* **2007**, 15, 108.

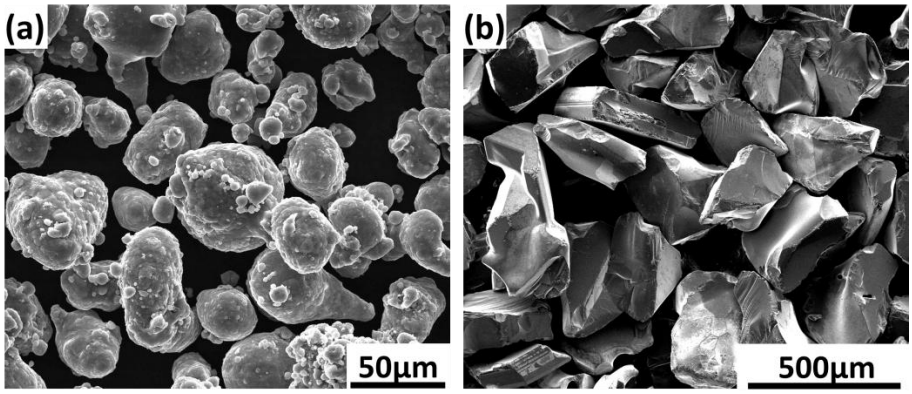


*Fig.1 SEM images showing morphologies of the starting materials: (a) Al powder and (b) SiC particles.*

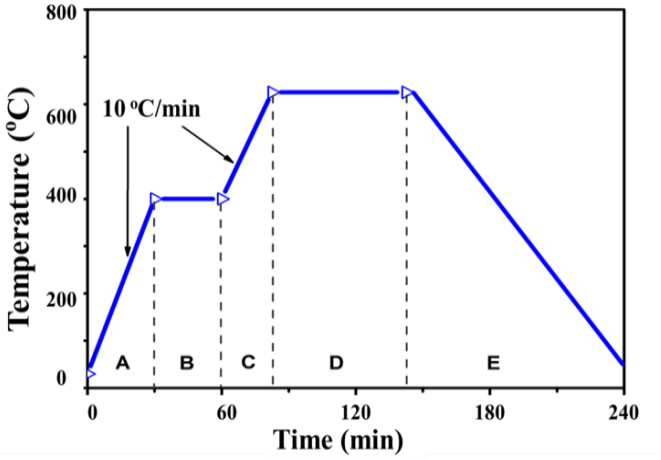


*Fig.2 A typical sintering cycle of vacuum hot pressing used in this work.*

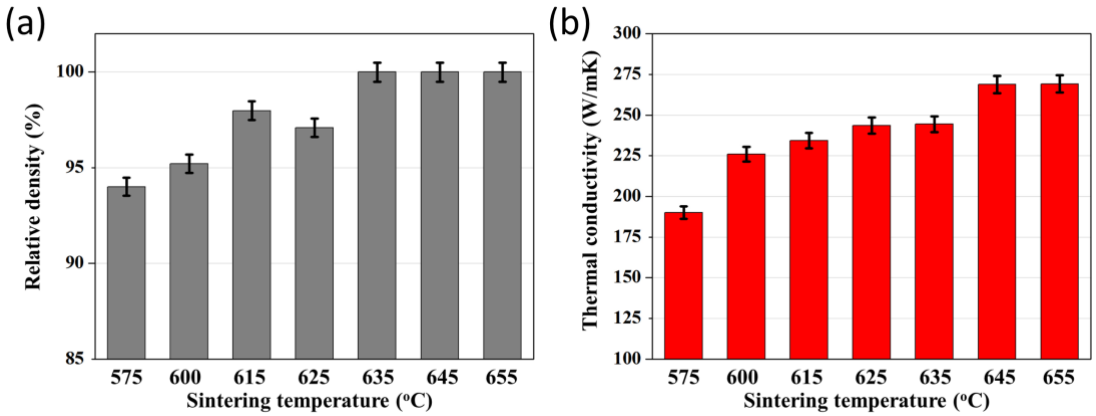


*Fig.3 (a) Relative density and (b) thermal conductivity of the 40 vol.% SiC/Al composites sintered at different temperatures from 575 to 655 °C for 60 min.*

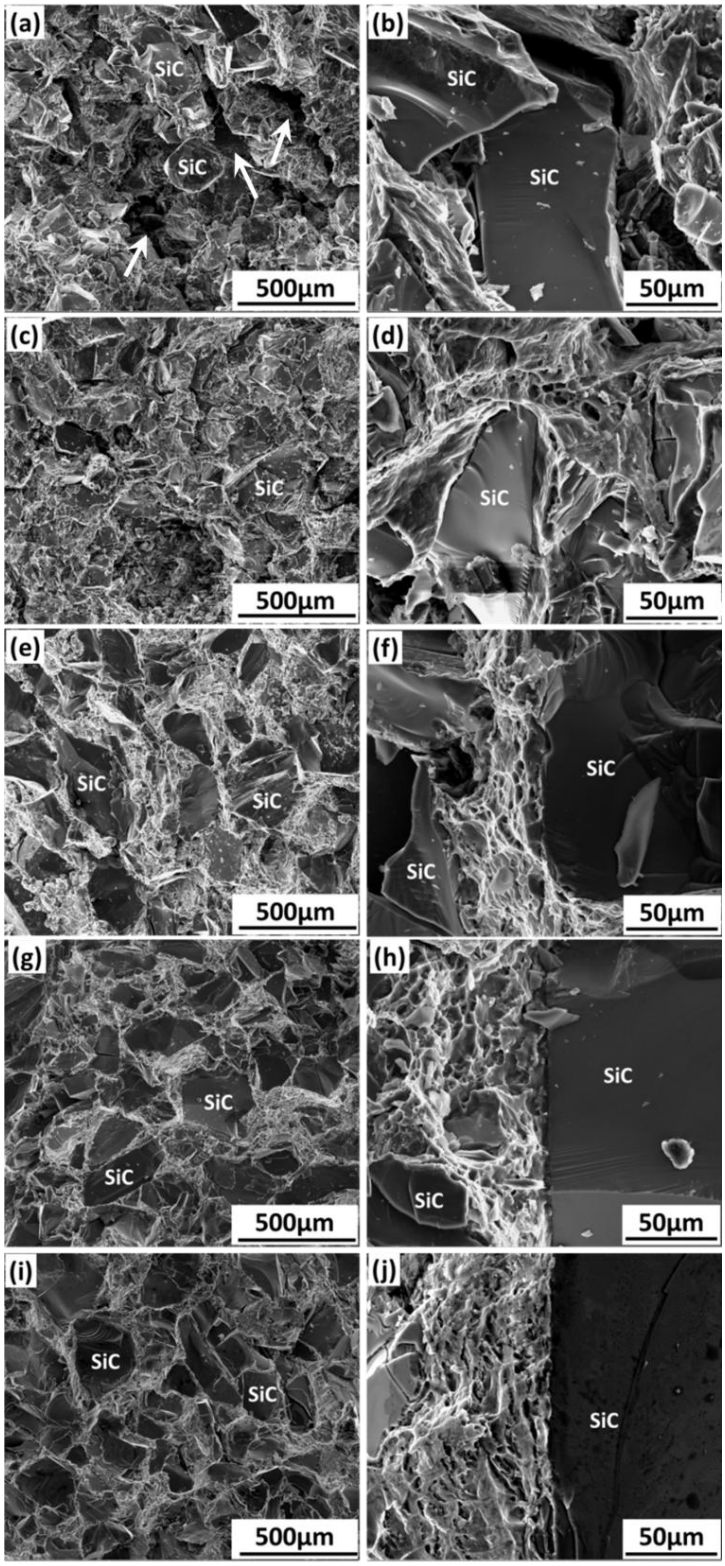


*Fig.4 SEM images showing fracture surfaces of the 40 vol.% SiC/Al composites sintered under the different conditions: (a)(b) at 575 °C for 60 min; (c)(d) at 600 °C for 60 min; (e)(f) at 625 °C for 60 min; (g)(h) at 655 °C for 60 min and (i)(j) at 655 °C for 180 min. Low-magnification images in (a), (c), (e), (g) and (i) showing an overview, while high-magnification images in (b), (d), (f), (g) and (i) highlighting the SiC/Al interface.*

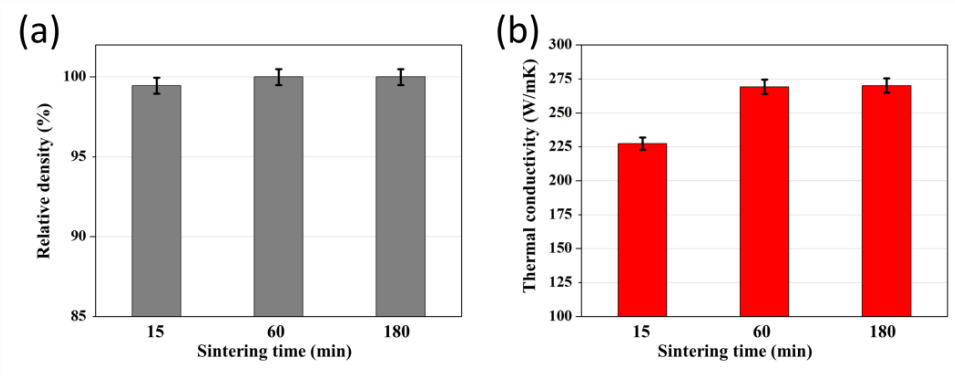


*Fig.5 (a) Relative density and (b) thermal conductivity of the 40 vol.% SiC/Al composites sintered at 655 $^{o}$C for different sintering times of 15, 60 and 180 min.*

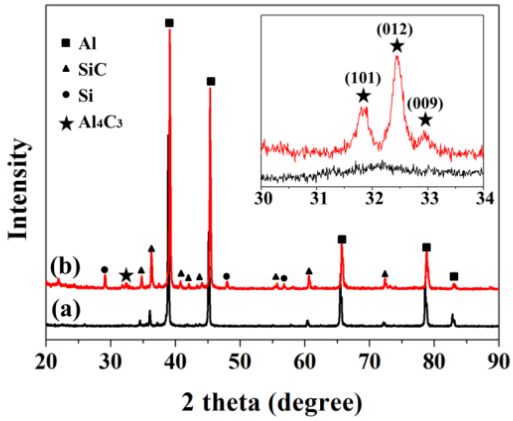


*Fig.6 Typical XRD patterns of the SiC/Al composites sintered at 655 $^{o}$C for (a) 60 min and (b) 180 min. Inset highlights the possible peaks of $Al_4C_3$: (101) (012) (009) peaks at 31.8$^{o}$, 32.5$^{o}$ and 32.9$^{o}$ of the pattern (b).*

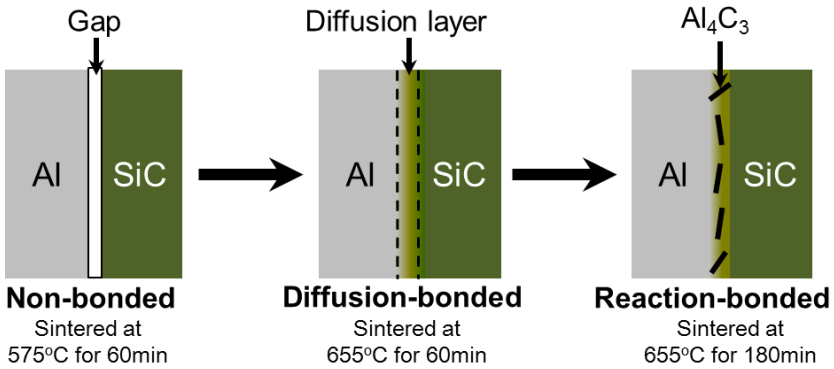


*Fig.7 Schematic illustration of the different stages of interface evolution in the SiC/Al composites and their corresponding technical parameters.*

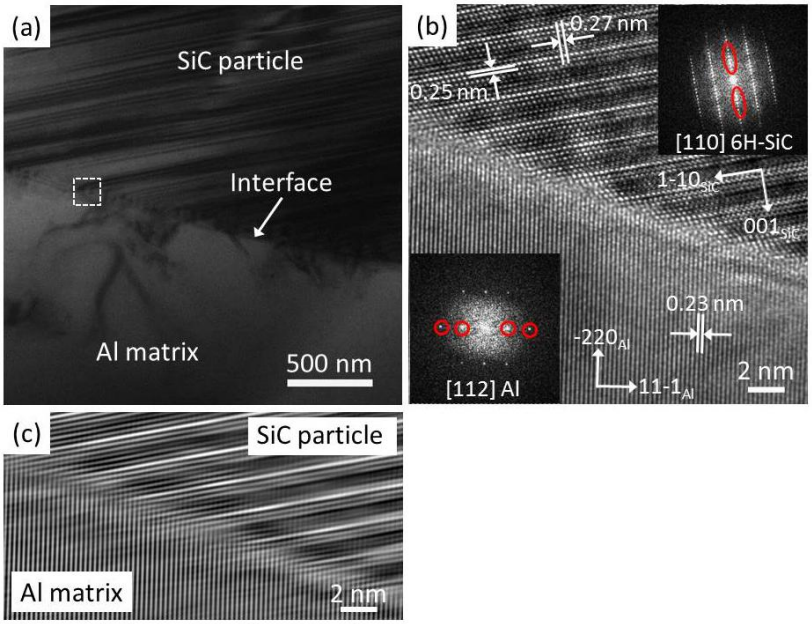


*Fig. 8 TEM analysis of the 40 vol.% SiC/Al composite sintered at 655 °C for 60 min. (a) TEM bright-field image showing a tightly-adhered interface between the SiC particle and the Al matrix; dark contrasts are mainly due to both sides being in good zone axis orientations, (b) HRTEM image of the interface included in the dotted line box shown in (a), insets in (b) are FFT patterns of [112] Al and [110] 6H-SiC and (c) Inverse FFT image highlighting a clean interface using circled reflections in the insets in (b), (see the text for more details).*

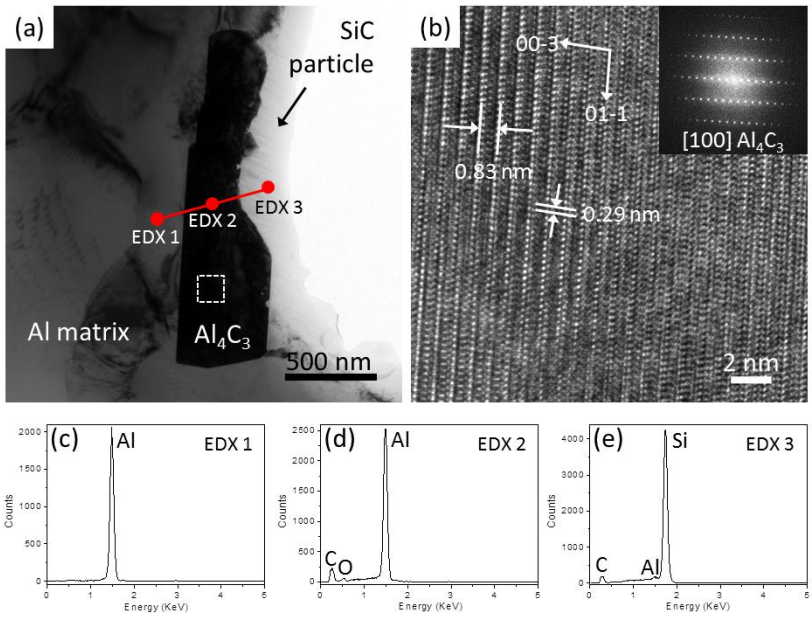


*Fig. 9 TEM analysis of the 40 vol.% SiC/Al composite sintered at 655 °C for 180 min. (a) TEM bright-field image showing an interface between the SiC particle and the Al matrix where the interfacial $Al_4C_3$ grain shows a dark contrast due to its good zone axis orientation; (b) HRTEM image of the area in the dotted line box shown in (a); (c), (d) and (e) EDX spectra recorded from the Al matrix, $Al_4C_3$ grain and SiC particle,*

*respectively. (see the text for more details).*

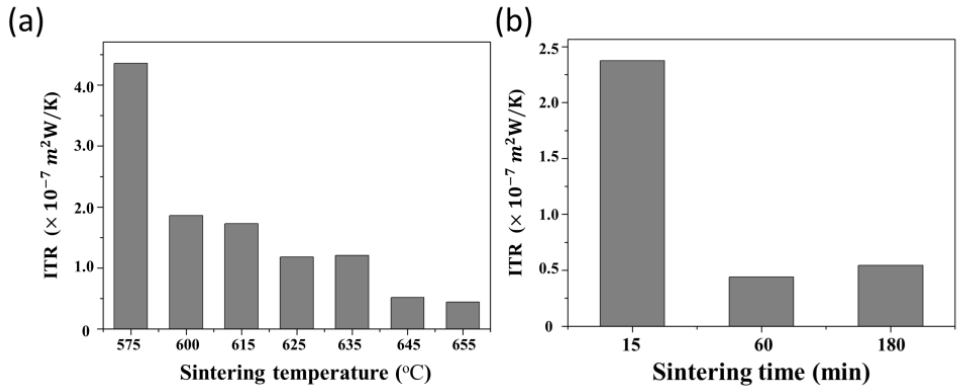


*Fig. 10 Theoretically calculated ITR of the 40 vol.% SiC/Al composites sintered: (a) at different temperatures from 575 to 655 °C for 60 min; (b) at 655 °C for different sintering times of 15, 60 and 180 min.*

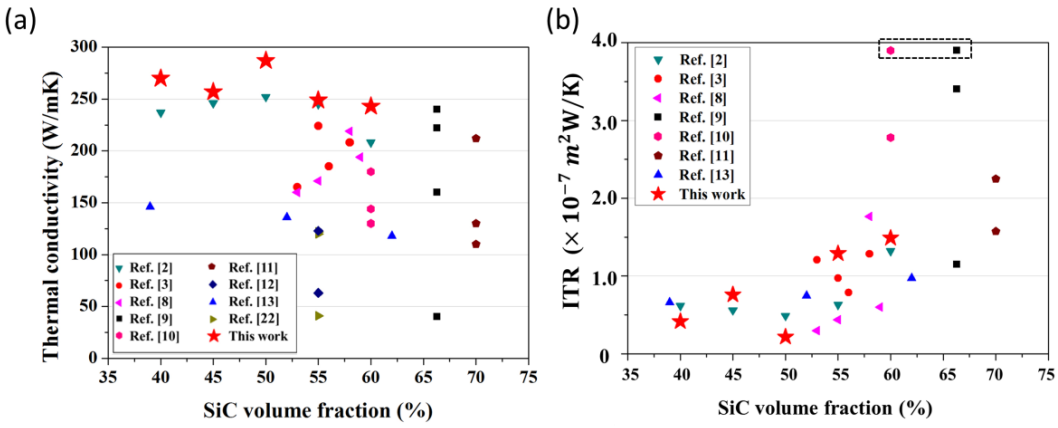


*Fig.11 Comparison of (a) thermal conductivity and (b) ITR values of the SiC/Al composites obtained in this work with those previously reported in the literatures. The dots in the dashed box of (b) represent ITR values ranging from 5.3×$10^{-7}$ to 7.2×$10^{-7}$ $m^2$W/K.*

Production Data

Click here to download Production Data: Prodaction Data.docx